NACA TN 2371 8775

TECH LIBRARY KAFB, NM
0065632

NATIONAL ADVISORY COMMITTEE FOR AERONAUTICS

TECHNICAL NOTE 2371

POSSIBLE APPLICATION OF BLADE BOUNDARY-LAYER CONTROL TO IMPROVEMENT OF DESIGN AND OFF-DESIGN PERFORMANCE OF AXIAL-FLOW TURBOMACHINES

By John T. Sinnette, Jr., and George R. Costello

Lewis Flight Propulsion Laboratory
Cleveland, Ohio

Washington
May 1951

AFMDC
TECH LIBRARY

TECH LIBRARY KAFB, NM

0065632

2116

NATIONAL ADVISORY COMMITTEE FOR AERONAUTICS

TECHNICAL NOTE 2371

POSSIBLE APPLICATION OF BLADE BOUNDARY-LAYER CONTROL TO IMPROVEMENT OF DESIGN AND OFF-DESIGN PERFORMANCE OF AXIAL-FLOW TURBOMACHINES

By John T. Sinnette, Jr., and George R. Costello

SUMMARY

A theoretical discussion of the application of blade boundary-layer control to increase the efficiency and the stage pressure ratio and to improve off-design performance of turbomachines is presented. A method based on the potential flow of a compressible fluid is developed for designing suction, or ejection, slotted blades having a prescribed velocity distribution along the blade and in the slot. The effect of the boundary layer on the design of the slot and the effect of ejecting gas at staghation pressures and temperatures different from free-stream values are discussed.

INTRODUCTION

Considerable research has been conducted on the application of boundary-layer control to isolated airfoils. These investigations prior to 1948 were summarized and evaluated by Sidney Goldstein in the Eleventh Wright Brothers Memorial Lecture (reference 1). The results of these investigations suggested certain possible applications to turbomachine (compressor and turbine) blading, which were theoretically investigated at the NACA Lewis laboratory during the summer of 1950 and are presented herein.

Boundary-layer control may be used either (a) to delay transition from a laminar to a turbulent boundary layer and thus reduce skin friction and heat transfer, or (b) to prevent or to delay boundary-layer separation and thereby increase the allowable blade loading and range of angles of attack.

The boundary-layer control to prevent separation may be obtained by either suction or ejection. The suction method appears, in general, to be the more efficient, but the ejection method would be necessary for use in conjunction with air-cooling of turbine blades.

Boundary-layer suction may be applied at a particular location through suction slots or distributed over an area by suction through a porous material. Although suction through porous walls has certain advantages, the practical difficulties, such as clogging and lack of strength, make it appear of somewhat dubious value for the blading of turbomachines. 2116

The applications of these methods of boundary-layer control for increasing the efficiency and the stage pressure ratio and improving the off-design performance of turbomachines are discussed. A potential-flow method of designing blades for boundary-layer control by prescribing the velocity distribution along the blade and in the slot is developed and compared with the theoretical results obtained for an unslotted blade with a velocity discontinuity. A discussion of the effect of the boundary layer on the design of the slot and the effect of ejecting gas at stagnation pressures and temperatures different from the free-stream values is also included.

SYMBOLS

The following symbols are used in this report:

$A,B,C,$ C_1,C_2,M	constants
$C(\zeta)$	function of ζ defined by equation (30)
C_L	blade lift coefficient
D	blade-profile drag
d	spacing of cascade
$F(\zeta)$	complex potential function (incompressible flow)
$f(\zeta)$	regular function of ζ
$g(\zeta)$	regular function of ζ
$H(\zeta)$	regular function of ζ
Im	imaginary part
$K(\theta)$	function of θ defined by equation (35)

2116

K_1	constant equal to $\dfrac{2q_1}{1+\sqrt{1+q_1^2}}$
K_2	constant equal to $\dfrac{2q_2}{1+\sqrt{1+q_2^2}}$
k	constant defined implicitly by equations (22) and (23)
L	blade-element lift
m	ratio of mass flow in slot to upstream mass flow
n	number determined by included trailing-edge angle of blade
p	pressure
$Q(s)$	auxiliary function of s
q	magnitude of dimensionless velocity in compressible-flow plane (ratio of actual velocity to stagnation velocity of sound)
R	region in ζ-plane defined by $\lvert\zeta\rvert \geq 1$
Re	real part
s	arc length along blade surface
u	rotor-blade-element velocity
$v(\theta)$	velocity on unit circle (incompressible flow)
w	auxiliary complex variable
$z = x + iy$	complex variable in compressible-flow plane (cascade plane)
α	angle of velocity in compressible flow (measured from positive x-axis)
β	angular location of sink on unit circle
Γ	circulation

ϵ	included trailing-edge angle of blade
$\zeta = \xi + i\eta$	complex variable in incompressible-flow plane (circle plane)
θ	circle angle in ζ-plane
λ	air angle relative to axial velocity
ρ	density
σ	blade-row solidity at mean radius
τ	variable of integration
φ	velocity potential
ψ	stream function

2116

Subscripts:

1	upstream of cascade
2	downstream of cascade
I	entrance to stator blade row
II	exit from stator blade row
III	exit from next rotor blade row
a	axial component
c	compressible flow
i	incompressible flow
m	relative mean velocity
n	leading edge (nose)
R	relative to rotor
S	relative to stator ("absolute" values)

t trailing edge (tail)

u upper surface

2116

The prime indicates a derivative.

APPLICATION OF BOUNDARY-LAYER CONTROL TO BLADING

Although boundary-layer control may well be applied to advantage on the hub and the casing of a turbomachine, the adequate analysis of such an application involves the consideration of three-dimensional boundary-layer flow (including the interaction of wall and blade boundary layers), which is outside the scope of the present investigation of blade boundary-layer control. Two-dimensional boundary-layer control on blading may be used to achieve several aims that are not entirely independent but which, for convenience, are separately discussed.

Increase of Blade Loading

As in the case of isolated airfoils, it is possible to increase the blade loading considerably by the use of boundary-layer control. This increase results from the prevention or the delay of flow separation and the resultant stalling of the blades, and the greatest gain, of course, can be obtained if the blades are specially designed for the use of the boundary-layer control so as to maintain high loading over most of the blade section. By use of boundary-layer control, a higher blade loading can be obtained for a given inlet Mach number without exceeding a given Mach number on the blade because the blade can be designed to have a uniformly high Mach number over a larger portion of the upper surface of the blade without flow separation. For the same reason, higher inlet Mach numbers can be used with a given loading without exceeding a given Mach number on the blade. The gain resulting from maintaining a high velocity over a larger portion of the upper surface may be materially reduced, however, by the increased velocity over the lower surface as a result of the practical requirement of thicker blades for boundary-layer control.

Improvement of Performance of Later Stage of Multistage Compressor

The largest gains from the increased loading obtainable with boundary-layer control on multistage axial-flow compressors would be in the later stages where the inlet Mach number is not the main limitation.

With conventional blading, the maximum pressure ratio per stage in a multistage compressor is obtained by increasing the axial component of velocity and maintaining an essentially symmetrical velocity diagram throughout in order to maintain the maximum allowable Mach number on all blade elements (reference 2). This increase in axial component of velocity can only be obtained by using a sufficiently large taper for the annular passage to more than compensate for the reduction in axial velocity due to the increase in density. The use of taper large enough to maintain constant relative Mach numbers, however, leads to very small passages in the later stages of high-pressure-ratio compressors and to high exit velocities (reference 3). The resultant narrow annular passage tends to produce low efficiencies in the later stages (reference 4) and the high exit velocities either produce large exit losses or require a long diffuser. For these reasons, most commercial compressors use much less taper than required to produce constant Mach number and consequently obtain relatively low Mach numbers and pressure ratios in the later stages. 2116

The drop-off in pressure ratio in the later stages due to this decrease in relative Mach number in the wider passage could be prevented, however, if the blade loading could be increased in these stages. Because of the lower Mach numbers, it should be possible to use considerably higher blade loading without obtaining excessive local Mach numbers on the blades. With conventional blading, however, the blade loading is limited by the early stall of the blades. The situation can be somewhat improved by the use of blades of high camber, but the gain is limited and the useful range of angles of attack may be reduced. Some further slight increase in pressure ratio can be obtained by the use of solidities higher than conventional limits of about 1.2, but the gain is generally obtained with some sacrifice in efficiency.

Effect of blade boundary-layer control. - A much greater increase in loading and stage pressure ratio should be possible through the use of boundary-layer control on the rotor and stator blades. The results from isolated airfoils indicate that there should be no difficulty in doubling the loading obtainable without boundary-layer control with a corresponding increase in pressure ratio. The effect of boundary-layer control on the stage efficiency is less easy to evaluate than its effect on stage pressure ratio. The profile drag-lift ratio should be decreased because of the large increase in lift coefficient possible without boundary-layer separation and because of the decreased profile drag resulting from reduced boundary-layer thickness behind the control slot. In addition, some improvement in efficiency might be expected from the fact that the velocity diagram theoretically most favorable to high profile efficiency for a given drag-lift ratio (symmetrical

2116

diagram with axial velocity equal to one-half rotor-blade velocity, references 2 and 5) can be approached more closely throughout a multistage compressor when a high stage pressure ratio is obtained by use of boundary-layer control on both rotor and stator blades than when it is obtained with conventional blades by varying the axial velocity to give a constant Mach number entering all blade rows. Thus, the profile stage efficiency should be higher than for conventional blades. On the other hand, "secondary-flow losses" may be increased if the empirical relations found for conventional blades (reference 6) apply to blades with boundary-layer control. It might be possible to reduce these losses, however, by proper variation of slot width along the blade span, by additional boundary-layer control at critical points, or by the choice of a suitable relation between the blade spacing and the amount of turning in the blade row.

In addition to the effect on internal aerodynamic efficiency, the power required for pumping the boundary-layer-control air must be considered in evaluating the over-all efficiency of the machine. If boundary-layer control were applied to all blade rows of a multistage compressor, the power used in pumping this air would undoubtedly have an appreciable effect on the over-all compressor efficiency. This statement applies even if the compressor itself is used to pump the boundary-layer air, as would generally be the case. Because of this pumping loss, it appears desirable to limit the boundary-layer control to the later stages where the largest gains are possible.

Boundary-layer control on stator blades. - Substantial gains can be obtained by applying the boundary-layer control only to the stator blades of the later stages, because it is generally necessary or desirable to remove the whirl of the air almost completely at the discharge from the compressor; this result can be obtained with a net gain in pressure ratio if the stator-blade loading can be substantially increased in the last few stages.

The manner in which this net gain in pressure ratio is obtained can be seen by examining typical velocity diagrams at the mean radius of a later stage with and without boundary-layer control on stators (fig. 1). The subscripts R and S indicate that the velocities are measured with respect to the rotor or stator reference frame, respectively, and the subscripts I, II, and III indicate the entrance to a stator row, the exit from the stator row, and the exit from the following rotor row, respectively. The same axial component of velocity q_a and rotor-blade-element velocity u are used in both cases. The absolute velocity $q_{I,S}$ entering the stator blades has been taken as the same in both cases, but the air is shown turned

through a much larger angle by the stators with boundary-layer control than by those without control, which results in absolute velocities leaving the stators $q_{II,S}$ that differ in magnitude and direction. The relative velocities entering the next row of rotor blades $q_{II,R}$ are therefore also different and much higher in the case where boundary-layer control is used on the stators. If the relative Mach number were 0.56 without boundary-layer control, it would be approximately 0.75 with control in this example. (The turning in the stators should be limited to give reasonable relative Mach numbers entering the following rotors.)

2116

The energy input and the total enthalpy rise are, by Euler's equation, proportional to the change in tangential component of velocity across the rotor Δq_R. The turning through the rotor blades in both cases of this example was determined by taking $C_L \sigma = 1$, where C_L is the lift coefficient and σ the solidity of the rotor row of blades. For the usual definition of lift coefficient used for compressors, this limitation on turning gives (reference 3)

$$C_L \sigma = 1 = \frac{2\left|\Delta q_R\right| \cos \lambda_{m,R}}{q_a\left(1 + \frac{D}{L} \tan \lambda_{m,R}\right)}$$

If the term involving D/L is neglected and q_a is constant, then

$$\left|\Delta q_R\right| \propto \frac{1}{\cos \lambda_{m,R}}$$

Hence, the total enthalpy rise, with this limitation on the turning in the rotor, is inversely proportional to the cosine of the angle between the mean relative velocity and the axis. Thus, the use of boundary-layer control on the stators, which allows this angle to be increased (fig. 1), gives higher total enthalpy rise and hence higher total-pressure ratio than without the control.

The process herein depicted may be repeated across several stages if desired, with the turning in the stators rather arbitrarily chosen to fit any desired conditions. For example, the stators may be designed to produce zero tangential velocity at the exit of the last row of rotor blades and thus to reduce the leaving losses to a minimum.

2116

Improvement of Turbine Performance

Boundary-layer control appears to have useful applications in conjunction with turbine-blade cooling. One of the most effective methods of cooling the trailing-edge region of turbine blades is by ejecting cooling air at or near the trailing edge of the blade. This ejected air can be used at the same time as an effective method of boundary-layer control for increasing the blade loading and thereby reducing the total blade area for a given power output. The reduction in blade-surface area may, in turn, be expected to reduce the amount of cooling required to maintain a given blade temperature. A somewhat different application of boundary-layer control would be made for turbines requiring very high work per pound of gas with limited rotor-blade speed, where negative reaction may be required. The flow through the turbine rotor is then similar to that through a typical compressor rotor and, if the blade loading is to be high, boundary-layer control may be required to prevent stalling of the blades. In this case, as in the more usual case, boundary-layer control by ejection can effectively be used in conjunction with blade cooling.

Improvement of Off-Design Performance of Turbomachines

In a multistage turbomachine designed for a high pressure ratio, the performance may be very poor when operating at equivalent speeds and weight flows far removed from the design values. The loss in efficiency is particularly serious in multistage axial-flow compressors when operating at below design speed, and is a result of extreme mismatching of the different stages. The first stages must operate at high angles of attack and may stall, whereas the last stages may be operating as a turbine (which reduces the over-all pressure obtained) or may even be subject to a negative stall of the blades.

Boundary-layer control may be used to improve this situation in several ways. In the first place, airfoils properly designed for boundary-layer control are capable of withstanding a much wider range of angles of attack than those without control (reference 7).

Another method of improving the off-design performance with boundary-layer control consists in varying the turning angle and the circulation for a given angle of attack by varying the amount of air sucked off for control. In general, increasing the suction through a slot near the tail edge on the upper surface increases the circulation (reference 8). This variation of the suction quantity can be used very effectively in the later stages of a multistage compressor where boundary-layer suction has already been suggested for improving the

design performance. Similar effects are obtained by varying ejection air in the ejection-control method for perfect fluid, but the analysis of the effect for actual fluid is not as clear.

The tendency of the later stages to perform little useful work at below-design speed due to a large reduction in angle of attack can be counteracted by an increase in the circulation by using increased suction at the reduced speeds. This benefit is obtained even when the suction is applied only to the stator blades because an increased turning through the stator blades results in an increased angle of attack on the following row of rotor blades and hence an increase in energy addition through the rotor blades. 2116

Boundary-layer control has not been particularly recommended for improving the design performance of the first stages of axial-flow compressors because of the high relative entrance Mach numbers required on these stages to obtain high mass flow and high rotor speed. The high Mach numbers require thin blades with relatively low loading, in which case the gain from boundary-layer control is small. It might be desirable, however, to employ boundary-layer control on these stages during the low-speed operation of the compressor in order to postpone the stalling of these blades at the high angles of attack at which they will then operate. Suction near the leading edge is fairly effective in postponing the stalling of thin airfoils (references 1 and 9 to 11) and might therefore be used to advantage in improving the performance of the first stages at low compressor speeds.

THEORY OF BLADE-DESIGN METHOD WITH SLOT

In reference 12, Lin shows that, if the pressure-density relation is

$$p = C_1 - \frac{C_2}{\rho} \tag{1}$$

then the compressible potential flow about a cascade of blades can be obtained by transforming an incompressible flow about the unit circle with the unit circle mapping into the cascade blades. This transformation is extended to give the compressible potential flow past a cascade of blades with suction or ejection slots in the blades by introducing a sink or source on the unit circle and a pole in the derivative of the mapping function at the same point.

The complex potential function $F(\zeta)$ for the incompressible flow about the unit circle due to complex sources at $\zeta = \pm e^{k}$ (k real

2116

and positive) and a sink or source on the circle at $\zeta = e^{i\beta}$ (β real) is

$$F(\zeta) = A \log_e(\zeta - e^{k}) + \bar{A} \log_e(\zeta - e^{-k}) +$$

$$B \log_e(\zeta + e^{k}) + \bar{B} \log_e(\zeta + e^{-k}) + 2 M \log_e(\zeta - e^{i\beta}) + C \tag{2}$$

where the bar indicates the complex conjugate, M is a real constant (positive for a source and negative for a sink) and A, B, and C are complex constants with

$$\text{Re } A = (- \text{Re } B - M) > 0 \tag{3}$$

The mapping between the z-plane and the ζ-plane defined by

$$dz = g(\zeta) \left(1 - \frac{e^{i\beta}}{\zeta}\right)^{-1} \left(\zeta^2 - e^{2k}\right)^{-1} d\zeta -$$

$$\frac{1}{4}\left[F'(\zeta)\right]^2 \left[g(\zeta)\right]^{-1} \left(1 - \frac{e^{i\beta}}{\zeta}\right) \left(\zeta^2 - e^{2k}\right) d\zeta \tag{4}$$

gives a compressible flow with a linear pressure-volume relation past a cascade of slotted blades with the velocity potential φ_c and stream function ψ_c in the z-plane given by

$$\varphi_c + i\psi_c = F(\zeta) \tag{5}$$

provided that $g(\zeta)$ is chosen to satisfy the following requirements:

$$\left.\begin{array}{ll}
\text{(a)} & g(\zeta) \text{ is regular in region } R \text{ defined by } |\zeta| \geq 1 \\
\text{(b)} & g(\zeta) \neq 0 \text{ in } R \text{ except where } F'(\zeta) = 0 \text{ (the order of the zero not to exceed 1)} \\
\text{(c)} & \oint dz = 0 \text{ along a path enclosing the unit circle and excluding the points } \zeta = \pm e^{k} \\
\text{(d)} & \left| F'(\zeta)\left[g(\zeta)\right]^{-1} \left(1 - \frac{e^{i\beta}}{\zeta}\right) \left(\zeta^2 - e^{2k}\right) \right| < 2 \text{ in } R
\end{array}\right\} \tag{6}$$

The magnitude q and direction α of the dimensionless velocity at any point in the z-plane are given by

$$\frac{2q}{1+\sqrt{1+q^2}}\,e^{-i\alpha} = \frac{F'(\zeta)(\zeta^2 - e^{2k})\left(1 - \frac{e^{i\beta}}{\zeta}\right)}{g(\zeta)} \tag{7}$$

2116

The proof that the differential equations for the velocity potential and stream function are satisfied and that the required boundary conditions are obtained in the z-plane by use of this transformation is the same as the proof given in reference 12. In the physical interpretation, part of the suction slot is considered as being ducted out along the span of the blade.

The preceding transformation can be extended to give additional suction, or ejection, slots on the blade by adding more sinks or sources on the unit circle and by putting poles in the derivative of the mapping function at the same points. In order to use this transformation in designing a cascade of blades with suction or ejection slots and a prescribed velocity distribution along the blade, the prescribed conditions are used to select a suitable incompressible flow about the unit circle and to determine the function $g(\zeta)$ in a manner similar to that used for a cascade of unslotted blades (references 13 and 14).

The prescribed conditions are the velocity distribution on the blade, the upstream velocity $q_1 e^{i\alpha_1}$, the downstream velocity $q_2 e^{i\alpha_2}$, and the ratio m of mass flow in the slot to inlet mass flow (m is negative for suction, positive for ejection). Because the prescribed velocity does not determine the circulation, either the circulation or the location of two equipotential points in the slot must also be assigned. The upstream and the downstream velocities are related by the continuity equation

$$\frac{1}{\sqrt{1+q_2^2}}\,q_2 \cos\alpha_2 = \frac{1}{\sqrt{1+q_1^2}}\,q_1\,(1+m)\cos\alpha_1 \tag{8}$$

Because the suction case and the ejection case differ only in the signs of M and m and in the location of the upper-surface stagnation point relative to the slot, only the suction case is considered in detail. For convenience, the axis of the cascade is taken along the y-axis and the flow is from right to left (fig. 2).

Flow in Circle Plane

The flow of an incompressible fluid about the unit circle is selected by determining the constants A, B, β, and k in the complex potential function $F(\zeta)$ from the given conditions. The constants A and B are determined from the upstream and the downstream velocities and the circulation; and β and k are determined by the range of potential between stagnation points.

Potential and circulation on blade. - The magnitude of the dimensionless velocity q along the surface of the blade and the slot is given as a function of the arc length $q = Q(s)$, where the total arc length is infinite and the trailing-edge stagnation point s_t has been taken at zero (fig. 3). If $Q(s)$ is defined by

$$\left.\begin{aligned} Q(s) &= -\,q(s) & -\infty \leq s \leq s_u \\ Q(s) &= q(s) & s_u \leq s \leq 0 \\ Q(s) &= -\,q(s) & 0 \leq s \leq s_n \\ Q(s) &= q(s) & s_n \leq s \leq +\infty \end{aligned}\right\} \tag{9}$$

where s_u and s_n are the upper surface and the nose stagnation points, respectively, then the velocity potential $\varphi_c(s)$ is given by

$$\varphi_c(s) = \int_0^s Q(s)\ ds \tag{10}$$

The circulation cannot be determined from the prescribed velocity because the integral

$$\int_{-\infty}^{+\infty} Q(s)\ ds$$

is an indeterminate, improper integral. Hence, either the circulation or the location (as a function of s) in the slot of two points a and b having the same potential must be assigned (figs. 2 and 3). When the location of points a and b is assigned,

$$\Gamma_c = \int_a^b Q(s)\ ds \tag{11}$$

With the circulation known, the spacing d of the cascade is given by

$$d = \frac{\Gamma_c}{q_1 \sin \alpha_1 - q_2 \sin \alpha_2} \tag{12}$$

2116

Determination of A, M, and B. - The value of d from equation (12) is used to evaluate A and B because the spacing is also given by the value of $\oint dz$ taken along a path around e^k or $-e^k$; that is,

$$id = \oint_{e^k} dz = -\oint_{-e^k} dz \tag{13}$$

Substituting dz from equation (4) in equation (13) and integrating give

$$\begin{aligned} id &= 2\pi i \left[\frac{g(e^k)}{2e^k\left(1 - e^{i\beta-k}\right)} + \frac{\bar{A}^2 2e^k\left(\overline{1 - e^{i\beta-k}}\right)}{4\,\bar{g}(e^k)}\right] \\ &= 2\pi i \left[\frac{A}{K_1} e^{i\alpha_1} + \frac{\bar{A}K_1 e^{i\alpha_1}}{4}\right] \end{aligned} \tag{14}$$

where

$$K_1 = \frac{2q_1}{1 + \sqrt{1 + q_1^{\,2}}}$$

The bracketed expression must be a real number, hence,

$$\operatorname{Im} A = -\frac{4+K_1^{\,2}}{4-K_1^{\,2}} \operatorname{Re} A \tan \alpha_1 \tag{15}$$

or

$$\operatorname{Im} A = -\sqrt{1 + q_1^{\,2}} \operatorname{Re} A \tan \alpha_1 \tag{16}$$

Substitution of Im A from equation (15) in equation (14) gives

$$\text{Re } A = \frac{4K_1 \left|\cos \alpha_1\right|}{4 + K_1^{\,2}} \frac{d}{2\pi} \tag{17}$$

or

$$\text{Re } A = \frac{q_1 \left|\cos \alpha_1\right|}{\sqrt{1 + q_1^{\,2}}} \frac{d}{2\pi} \tag{18}$$

Hence, A is completely determined by equations (15) and (17) or (16) and (18).

The ratio m (which is negative in the suction case) of the mass flow removed to total flow is given and consequently

$$M = m \text{ Re } A \tag{19}$$

Equation (3) may be written

$$\text{Re } B = - \text{Re } A - M \tag{20}$$

and Re B is thus obtained from the preceding values of Re A and M. The value of Im B is determined from the spacing by

$$id = -\oint_{-e^k} dz = - 2\pi i \left(\frac{B}{K_2} e^{i\alpha_2} + \frac{\overline{B}K_2 e^{i\alpha_2}}{4} \right)$$

where

$$K_2 = \frac{2q_2}{1 + \sqrt{1 + q_2^{\,2}}}$$

Therefore

$$\text{Im } B = -\frac{4+K_2^{\,2}}{4-K_2^{\,2}} \text{ Re } B \tan \alpha_2$$

$$= -\sqrt{1 + q_2^{\,2}} \text{ Re } B \tan \alpha_2 \tag{21}$$

and B is completely known from equations (20) and (21).

Determination of k and β. - After A, M, and B are known, k and β are determined by the condition that the maximums and the minimums of the potential on the circle must equal those of the potential on the blade; that is,

$$\varphi_c(s_u) - \varphi_c(0) = F\left(e^{i\theta_u}\right) - F\left(e^{i\theta_t}\right) \tag{22}$$

$$\varphi_c(s_n) - \varphi_c(0) = F\left(e^{i\theta_n}\right) - F\left(e^{i\theta_t}\right) \tag{23}$$

where θ_u, θ_t, and θ_n are the upper surface, the trailing edge, and the nose stagnation points, respectively. This system of equations in k and β always has solutions, but the equations cannot be solved analytically and some numerical method must be used. One method is to obtain a plot of k as a function of β for values that satisfy equation (22) by assigning a few values to β and determining the corresponding values of k. Similarly, obtain a plot of k as a function of β for values that satisfy equation (23). The intersection of these curves gives the desired values of k and β.

With k and β determined, the flow about the circle is known. The potential $\varphi_i(\theta)$ on the circle is

$$\varphi_i(\theta) = \text{Re } F(e^{i\theta}) = -2 \text{ Re } A \tanh^{-1} \frac{\cos \theta}{\cosh k} +$$

$$(\text{Im } A + \text{Im } B) \tan^{-1} \frac{\tan \theta}{\tanh k} + (\text{Im } A - \text{Im } B) \tan^{-1} \frac{\sin \theta}{\sinh k} +$$

$$M \log_e \frac{1 - \cos (\theta - \beta)}{\cosh k + \cos \theta} + \text{Re } C \tag{24}$$

2116

and Re C is chosen to make $\varphi_i(\theta_t) = 0$. The angle convention is

$$-\frac{\pi}{2} < \tan^{-1}\frac{\sin\theta}{\sinh k} < \frac{\pi}{2}$$

and $\tan^{-1}\frac{\tan\theta}{\tanh k}$ is taken in the same quadrant and direction as θ.

The velocity on the circle $v(\theta)$ is

$$v(\theta) = \frac{2}{\cosh 2k - \cos 2\theta}\Big[2\,\mathrm{Re}\,A \sin\theta \cosh k + (\mathrm{Im}\,A - \mathrm{Im}\,B)\cos\theta \sinh k + (\mathrm{Im}\,A + \mathrm{Im}\,B)\sinh k \cosh k\Big] + M\left(\mathrm{ctn}\,\frac{\theta-\beta}{2} + \frac{\sin\theta}{\cosh k + \cos\theta}\right) \tag{25}$$

Function $g(\zeta)$

The function $g(\zeta)$ can be computed for points on the unit circle by using the prescribed velocity on the blade and the velocity on the circle to determine the real part of $g(\zeta)$. The imaginary part could then be computed by Poisson's integral. Because of the restriction imposed by the prescribed conditions, $g(\zeta)$ is obtained in a slightly different manner, as shown in the following sections.

Blade with pointed trailing edge. - If the blade is to have a pointed trailing edge, then $g(\zeta)$ must vanish at the trailing-edge stagnation point on the circle, $\zeta = e^{i\theta_t}$. Hence, $g(\zeta)$ may be written as

$$g(\zeta) = \left(1 - \frac{e^{i\theta_t}}{\zeta}\right)^n e^{f(\zeta)} \tag{26}$$

where $f(\zeta)$ is regular on and outside the unit circle and

$$n = 1 - \frac{\epsilon}{\pi} \tag{27}$$

where ϵ is the included trailing-edge angle of the blade.

2116

Values of $g(\pm e^k)$. - Because the velocities upstream and downstream are prescribed, the values of $g(\zeta)$ at $\zeta = \pm e^k$ are determined from equation (7):

$$\left.\begin{aligned} g(e^k) &= \frac{2Ae^{i\alpha_1}\left(e^k - e^{i\beta}\right)}{K_1} \\ g(-e^k) &= \frac{-2Be^{i\alpha_2}\left(e^k + e^{i\beta}\right)}{K_2} \end{aligned}\right\} \tag{28}$$

In order that $g(\zeta)$ have these values, $f(\zeta)$ is written in the form

$$f(\zeta) = C(\zeta) + \frac{\left(e^{2k} - \zeta^2\right)\left(\zeta^2 - e^{-2k}\right)}{\zeta^2} H(\zeta) \tag{29}$$

where

$$\begin{aligned} C(\zeta) = {} & \frac{1}{2}\left(1 + \frac{e^k}{\zeta}\right)\log_e \frac{2A\left(e^k - e^{i\beta}\right)e^{i\alpha_1}}{K_1\left(1 - e^{i\theta_t - k}\right)^n} + \\ & \frac{1}{2}\left(1 - \frac{e^k}{\zeta}\right)\log_e \frac{-2B\left(e^k + e^{i\beta}\right)e^{i\alpha_2}}{K_2\left(1 + e^{i\theta_t - k}\right)^n} \end{aligned} \tag{30}$$

and $H(\zeta)$ is regular on and outside the unit circle with

$$\lim_{\zeta \to \infty} \zeta H(\zeta) = 0 \tag{31}$$

This restriction on $H(\zeta)$ is imposed by the regularity of $f(\zeta)$. By use of equations (26) and (29),

$$g(\zeta) = \left(1 - \frac{e^{i\theta_t}}{\zeta}\right)^n e^{\left[C(\zeta) + \left(e^{2k} - \zeta^2\right)\left(\zeta^2 - e^{-2k}\right)\zeta^{-2} H(\zeta)\right]} \tag{32}$$

and $g(\zeta)$ will be known when $H(\zeta)$ is determined. For the computation of the blade shape, only the values of $g(\zeta)$ on the circle are needed.

2116

Determination of $\operatorname{Re} H(\zeta)$ on circle. - By equation (5), the potentials $\varphi_c(s)$ and $\varphi_1(\theta)$ are equal at corresponding points. Thus, by matching these potentials, a correspondence is established between points along the blade arc length and the circle angle: $s = s(\theta)$. By use of this correspondence, the magnitude of the velocity prescribed along the blade is obtained as a function of the circle angle: $q = q(\theta)$. Hence, from equation (7),

$$\frac{2\,q(\theta)}{1+\sqrt{1+q^2(\theta)}} = \frac{\left|F'(e^{i\theta})(e^{i2\theta} - e^{2k})\left(1 - e^{i(\beta-\theta)}\right)\right|}{\left|g(e^{i\theta})\right|} \tag{33}$$

Substituting $g(\zeta)$ from equation (32) with $\zeta = e^{i\theta}$ and replacing $\left|F'(e^{i\theta})\right|$ by the velocity $v(\theta)$ (equation (25)) in equation (33) give

$$\frac{2q(\theta)}{1+\sqrt{1+q^2(\theta)}} = \frac{e^k\left|v(\theta)\right|(2\cosh 2k - 2\cos 2\theta)^{1/2}\,2\left|\sin\frac{\beta-\theta}{2}\right|}{\left[2-2\cos(\theta_t-\theta)\right]^{n/2}\,e^{\left[\operatorname{Re} C(e^{i\theta}) + (2\cosh 2k - 2\cos 2\theta)\operatorname{Re} H(e^{i\theta})\right]}}$$

or

$$\operatorname{Re} H(e^{i\theta}) = \frac{\log_e \dfrac{\left|v(\theta)\right|(2\cosh 2k - 2\cos 2\theta)^{1/2}\,2\left|\sin\frac{\beta-\theta}{2}\right|}{K(\theta)\left[2-2\cos(\theta_t-\theta)\right]^{n/2}} - \operatorname{Re} C(e^{i\theta}) + k}{2\cosh 2k - 2\cos 2\theta} \tag{34}$$

where

$$K(\theta) = \frac{2\,q(\theta)}{1+\sqrt{1+q^2(\theta)}} \tag{35}$$

Restrictions on $\operatorname{Re} H(e^{i\theta})$. - By equation (31),

$$\lim_{\zeta\to 0} \zeta\, H(\zeta) = 0$$

hence $H(\zeta)$ must have the form

$$H(\zeta) = \frac{h_2}{\zeta^2} + \frac{h_3}{\zeta^3} + \ldots$$

2116

(where $h_2, h_3, \ldots$ are complex constants) which for points on the unit circle becomes

$$H(e^{i\theta}) = \text{Re } H(e^{i\theta}) + i \text{ Im } H(e^{i\theta}) = \frac{h_2}{e^{i2\theta}} + \frac{h_3}{e^{i3\theta}} + \ldots$$

$$= \sum_{j=2}^{\infty} (\text{Re } h_j \cos j\theta + \text{Im } h_j \sin j\theta) +$$

$$i \sum_{j=2}^{\infty} (\text{Im } h_j \cos j\theta - \text{Re } h_j \sin j\theta) \tag{36}$$

Consequently,

$$\int_0^{2\pi} \text{Re } H(e^{i\theta}) \, d\theta = 0 \tag{37}$$

$$\int_0^{2\pi} \text{Re } H(e^{i\theta}) \cos \theta \, d\theta = 0 \tag{38}$$

$$\int_0^{2\pi} \text{Re } H(e^{i\theta}) \sin \theta \, d\theta = 0 \tag{39}$$

The values of $\text{Re } H(e^{i\theta})$ from equation (34) must satisfy equations (37) to (39). If these equations are not satisfied, the values of $\text{Re } H(e^{i\theta})$ must be adjusted until the conditions are satisfied, which modifies the prescribed velocity. Methods for adjusting $\text{Re } H(e^{i\theta})$ are given in reference 14. These adjustments must be made in such a manner that $\text{Re } H(e^{i\theta})$ still satisfies the restriction imposed by equation (6d), which may be written in the form

$$e^{\left[(2 \cosh 2k - 2 \cos 2\theta) \operatorname{Re} H(e^{i\theta})\right]}$$

$$> \frac{e^{k}\left|v(\theta)\right| (2 \cosh 2k - 2 \cos 2\theta)^{1/2} \left|\sin \frac{\beta-\theta}{2}\right|}{\left[2 - 2 \cos (\theta_t-\theta)\right]^{n/2} e^{R\dot{e}\, C(e^{i\theta})}} \tag{40}$$

Determination of $\operatorname{Im} H(e^{i\theta})$. - After obtaining $\operatorname{Re} H(e^{i\theta})$, which satisfies equations (37) to (40), the function $\operatorname{Im} H(e^{i\theta})$ is given by Poisson's integral

$$\operatorname{Im} H(e^{i\theta}) = \frac{1}{2\pi} \int_0^{2\pi} \operatorname{Re} H(e^{i\tau}) \cot \frac{\tau-\theta}{2}\, d\tau \tag{41}$$

where the constant term in the integral has been taken as zero so that

$$\int_0^{2\pi} \operatorname{Im} H(e^{i\theta})\, d\theta = 0$$

as required by equation (36). Hence, $H(e^{i\theta})$ is now determined by

$$H(e^{i\theta}) = \operatorname{Re} H(e^{i\theta}) + i \operatorname{Im} H(e^{i\theta})$$

and substitution of these values of $H(e^{i\theta})$ in equation (32) gives the values of $g(\zeta)$ for points on the circle $\zeta = e^{i\theta}$.

Blade Coordinates

From the preceding values of $g(e^{i\theta})$, the blade coordinates are obtained by integration around the circle of equation (4); that is,

$$z = \int g(e^{i\theta}) \left[1 - e^{i(\beta-\theta)}\right]^{-1} (e^{2i\theta} - e^{2k})^{-1}\, d(e^{i\theta}) -$$

$$\frac{1}{4}\int \sqrt{\left[F'(e^{i\theta})\right]^2 \left[g(e^{i\theta})\right]^{-1} \left[1 - e^{i(\beta-\theta)}\right] (e^{2i\theta} - e^{2k})}\, d(e^{i\theta})$$

which, on replacing $F'(e^{i\theta})$ by $v(\theta)\ e^{-i(\theta+\frac{\pi}{2})}$ and writing

$$g(e^{i\theta}) = g_1(\theta)\ e^{ig_2(\theta)}$$

reduces to

$$z = \int \left\{ g_1(\theta) \left[1 - e^{i(\beta-\theta)}\right]^{-1} \left(e^{2i\theta} - e^{2k}\right)^{-1} - \frac{v(\theta)^2}{4\ g_1(\theta)} \overline{\left[1 - e^{i(\beta-\theta)}\right]}\ \overline{\left(e^{2i\theta} - e^{2k}\right)} \right\} e^{i(\theta + \frac{\pi}{2} + g_2)}\ d\theta \tag{42}$$

ILLUSTRATIVE EXAMPLE

In order to compare an example of a slotted blade with a previously computed unslotted, Griffith type blade, which had an abrupt decrease in the upper surface velocity (figs. 4 and 5), the same upstream velocity, turning angle, spacing, and circulation were chosen for this example:

$$q_1 = 0.68215$$

$$\alpha_1 = 135^\circ$$

$$\alpha_2 = 180^\circ$$

$$\Gamma = 0.5058$$

$$d = 1.0488$$

and a similar velocity distribution was prescribed along the blade. The amount of suction was taken to be 1 percent of the mass flow ($m = -0.01$). The integrals in equations (36) to (40) were evaluated by the methods given in reference 14. In order to obtain sufficient accuracy in the neighborhood of the slot, when the coefficients given in reference (14) are used, $\mathrm{Re}\ H(e^{i\theta})$ was written in the form

$$\mathrm{Re}\ H(e^{i\theta}) = \mathrm{Re}\ H_1(e^{i\theta}) + \mathrm{Re}\ H_2(e^{i\theta})$$

where

$$\text{Re } H_1(e^{i\theta}) = 0 \qquad \text{for } \beta - 20^\circ < \theta < \beta + 20^\circ$$

2116.

$$\text{Re } H_1(e^{i\theta}) = \text{Re } H(e^{i\theta}) \qquad \text{for all other values of } \theta$$

$$\text{Re } H_2(e^{i\theta}) = \text{Re } H(e^{i\theta}) \qquad \text{for } \beta - 20^\circ < \theta < \beta + 20^\circ$$

$$\text{Re } H_2(e^{i\theta}) = 0 \qquad \text{for all other values of } \theta$$

The integrals involving $\text{Re } H_1(e^{i\theta})$ were evaluated using 80 equally spaced values of θ and the integrals involving $\text{Re } H_2(e^{i\theta})$ were obtained by conformally mapping the unit circle onto a unit circle by

$$w = \frac{\zeta - 0.95\, e^{i\beta}}{0.95\, e^{-i\beta} \cdot \zeta - 1}$$

and using 80 equally spaced values of the new circle angle.

Adjustments to $\text{Re } H(e^{i\theta})$ changed the prescribed velocity somewhat and the final velocity distribution is shown in figure 6. The computed blade shape is given in figure 7. The trailing edge of the slot has a very small radius of curvature and, in order to obtain a more practical blade, the velocity was represcribed in this neighborhood (fig. 8) and also a lower velocity was prescribed in the slot. The resulting velocity distribution and blade are shown in figures 9 and 10, respectively.

DISCUSSION OF SLOT DESIGN METHOD

The design method with a slot directly applies to potential compressible flow with a linear pressure-volume relation. The interpretation given in reference 14, which consists in multiplying the velocities for a linearized pressure-volume relation by a constant factor, can be used to obtain an approximate solution for a gas obeying the usual isentropic relations and satisfying irrotationality and continuity between upstream and downstream flow. The limitation to potential flow, however, is a more serious restriction because most of the slot flow is boundary-layer flow with total pressures and temperatures

differing from those of the main flow. Thus, the method cannot be directly applied to actual flows. A reasonable method of allowing for the boundary layer in the case of suction would be to displace the upstream boundary of the slot by a little more than the displacement thickness of the boundary layer in order to allow the slot to pass the desired mass flow.

2116

The modification of the potential-flow solution to represent actual ejection control is more complicated. Even without the effect of viscosity, the ejection process may differ from the potential-flow solution because the total pressure and temperature of the ejected gas need not be the same as that of the main flow. Then a discontinuity in both temperature and velocity (but not pressure) would generally be produced where the two flows come together. When viscosity is considered, the discontinuity surface disappears and will be replaced by a wake region where the boundary layers from the blade and the upstream side of the slot merge.

The nonviscous case can be analyzed approximately on a one-dimensional basis by applying Bernoulli's equation to stream tubes on either side of the surface of discontinuity and making use of the continuity of pressure across the surface of discontinuity. The viscous case is considerably more difficult and must be treated by boundary-layer techniques that are beyond the scope of the present investigation. The general approach to obtaining the actual flow with ejection would be, however, to start with the potential-flow solution obtained in the present report and then to modify it in succession to take account of different total pressures and temperatures and then modify that solution to account for viscous and heat-transfer effects.

For low suction or ejection flows (1 percent or less of upstream flow), the blade shape obtained by the method of reference 14 using a discontinuity in the velocity is essentially the same as the blade shape obtained by the method of this report except in the vicinity of the slot. Consequently, considerable time could be saved in designing blades with low suction or ejection flows by using the method of reference 14 to obtain the general blade shape and then fairing into the blade a previously calculated (or known) slot that is capable of handling the flow.

Lewis Flight Propulsion Laboratory,
National Advisory Committee for Aeronautics,
Cleveland, Ohio, December 13, 1950.

2116

REFERENCES

1. Goldstein, Sidney: Low-Drag and Suction Airfoils. Jour. Aero. Sci., vol. 15, no. 4, April 1948, pp. 189-214; discussion, pp. 215-220.

2. Sinnette, John T., Jr.: Analysis of Effect of Basic Design Variables on Subsonic Axial-Flow-Compressor Performance. NACA Rep. 901, 1948.

3. Wu, Chung-Hua, Sinnette, John T., Jr., and Forrette, Robert E.: Theoretical Effect of Inlet Hub-Tip-Radius Ratio and Design Specific Mass Flow on Design Performance of Axial-Flow Compressor. NACA TN 2068, 1950.

4. Eckert, B.: The Influence of Physical Dimensions (Such as Hub: Tip, Ratio, Clearance, Blade Shape) and Flow Conditions (Such as Reynolds Number and Mach Number) on Compressor Characteristics. Part A - Summary of the Results of Research on Axial Flow Compressors at the Stuttgart Research Institute for Automobiles and Engines. W.A.C. Eng. Trans. No. 22, Wright Aero. Corp. (Vol. 3 of series of articles on compressor and fan design, written by German engineers, coordinated by Code 338, BuShips, Navy Dept. (Washington, D.C.), May 1946.)

5. Sinnette, John T., Jr., Schey, Oscar W., and King, J. Austin: Performance of NACA Eight-Stage Axial-Flow Compressor Designed on the Basis of Airfoil Theory. NACA Rep. 758, 1943.

6. Howell, A. R.: Fluid Dynamics of Axial Compressors. War Emergency Issue No. 12 pub. by Inst. Mech. Eng. (London), 1945. (Reprinted in U.S. by A.S.M.E., Jan. 1947, pp. 441-452.)

7. Glauert, M. B.: The Design of Suction Airfoils with a Very Large C_L-Range. R. & M. No. 2111, British A.R.C., Nov. 1945.

8. Smith, C. B.: A Solution for the Lift and Drag of Airfoils with Air Inlets and Suction Slots. Jour. Aero. Sci., vol. 16, no. 10, Oct. 1949, pp. 581-589.

9. Lighthill, M. J.: A Theoretical Discussion of Wings with Leading-edge Suction. R. & M. No. 2162, British A.R.C., May 1945.

10. Thwaites, B.: A Theoretical Discussion of High-lift Aerofoils with Leading-edge Porous Suction. R. & M. No. 2242, British A.R.C., July 1946.

11. Nuber, Robert J., and Needham, James R., Jr.: Exploratory Wind-Tunnel Investigation of the Effectiveness of Area Suction in Eliminating Leading-Edge Separation over an NACA 64_1A212 Airfoil. NACA TN 1741, 1948.

12. Lin, C. C.: On the Subsonic Flow through Circular and Straight Lattices of Airfoils. Jour. Math. and Phys., vol. XXXVIII, no. 2, July 1949, pp. 117-130.

13. Costello, George R.: Method of Designing Cascade Blades with Prescribed Velocity Distributions in Compressible Potential Flows. NACA Rep. 978, 1950. (Formerly NACA TN's 1970 and 1913.)

14. Costello, George R., Cummings, Robert L., and Sinnette, John T., Jr.: Detailed Computational Procedure for Design of Cascade Blades with Prescribed Velocity Distributions in Compressible Potential Flows. NACA TN 2281, 1951.

2116

2116

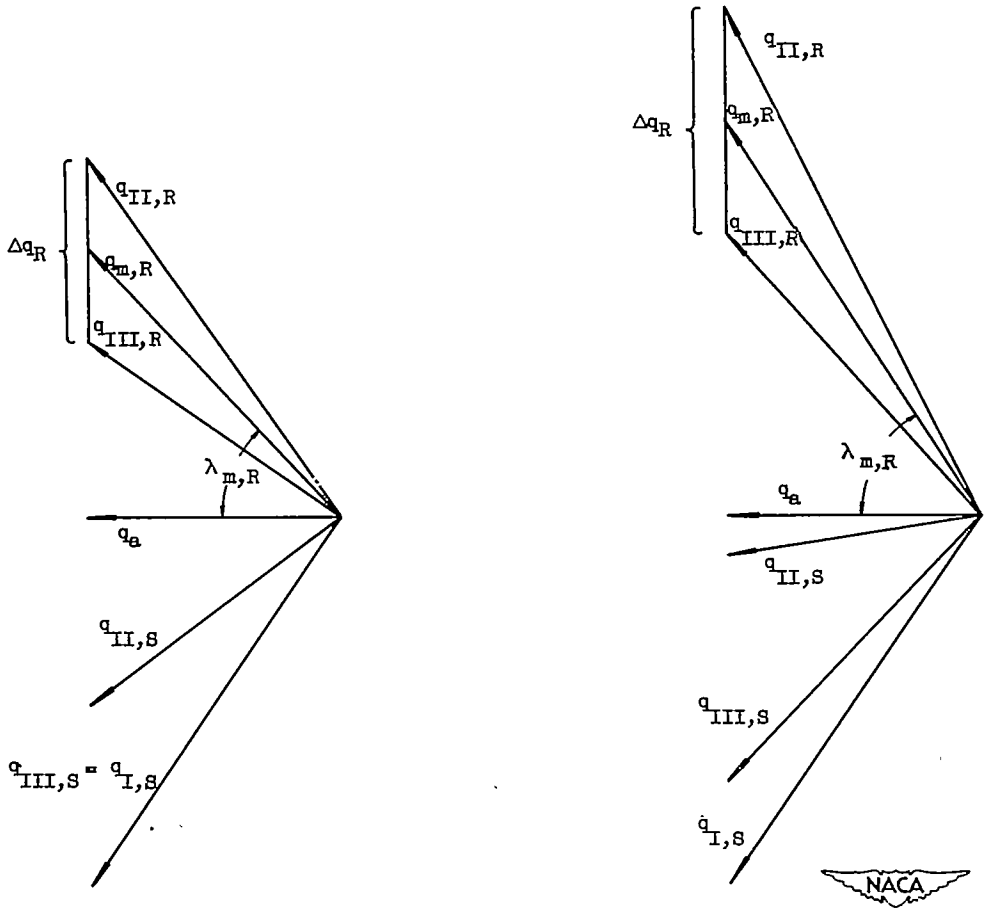

(a) Without boundary-layer control.

(b) With boundary-layer control.

Figure 1. - Velocity diagrams at mean radius of later stage of multistage axial-flow compressor with and without boundary-layer control on stator blades.

2116

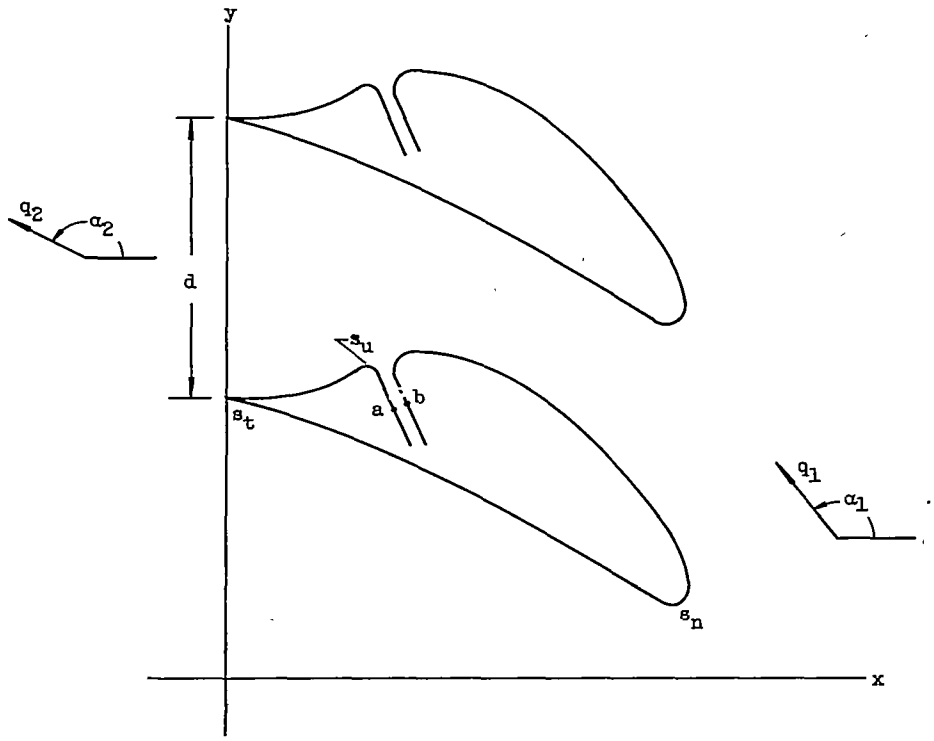

Figure 2. - Cascade in z-plane.

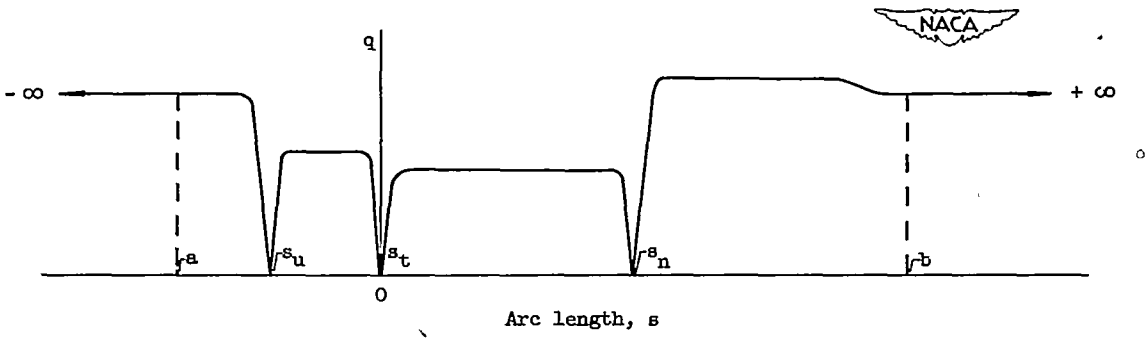

Figure 3. - Velocity distribution on cascade blade.

2116

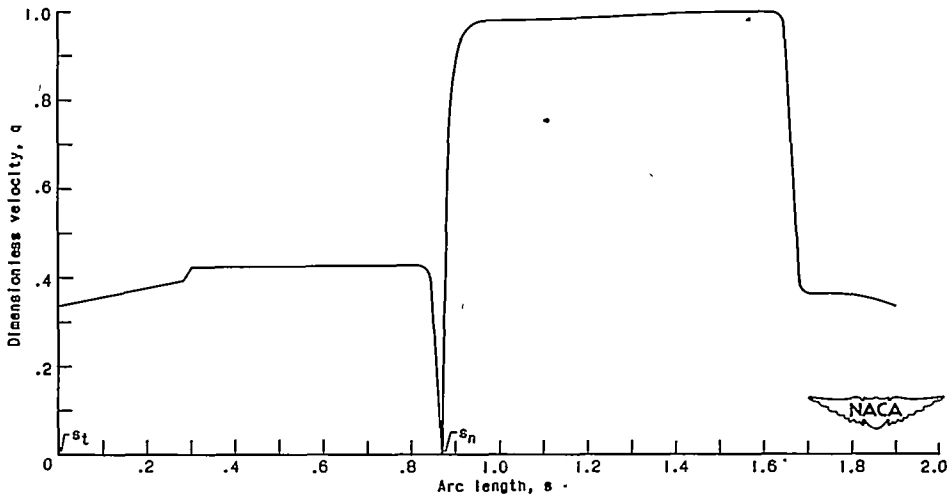

Figure 4. - Velocity distribution for Griffith type blade.

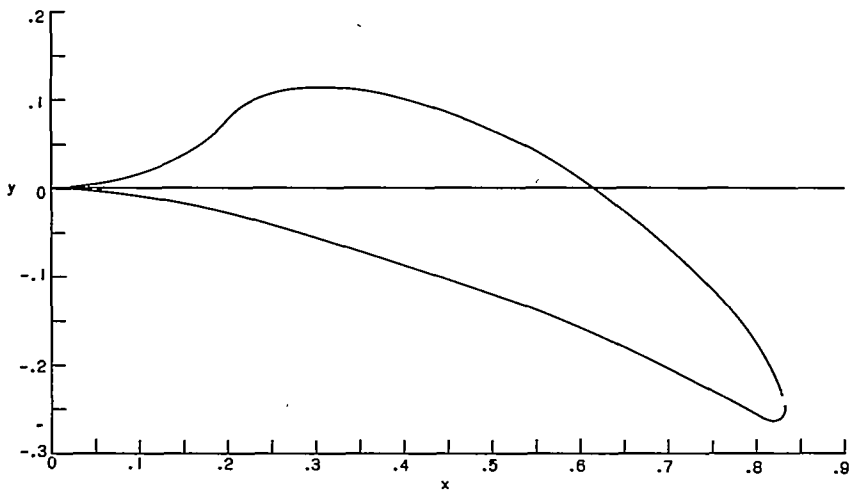

Figure 5. - Griffith type blade. Cascade spacing, d, 1.0488; upstream of cascade: magnitude of dimensionless velocity, q_1, 0.68215; angle of velocity, α_1, 135°; downstream of cascade: magnitude of dimensionless velocity, q_2, 0.43445; angle of velocity, α_2, 180°.

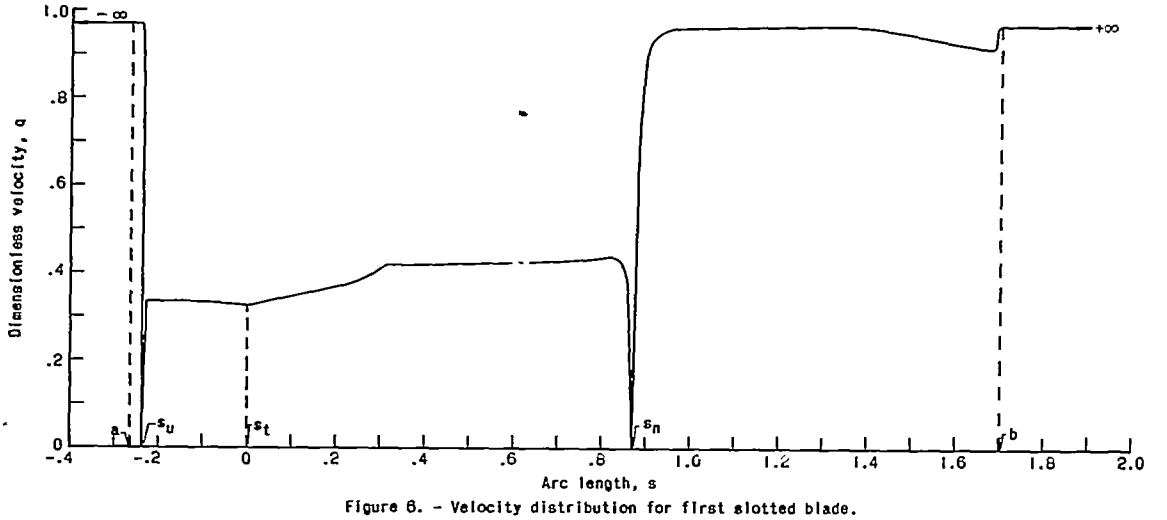

Figure 6. - Velocity distribution for first slotted blade.

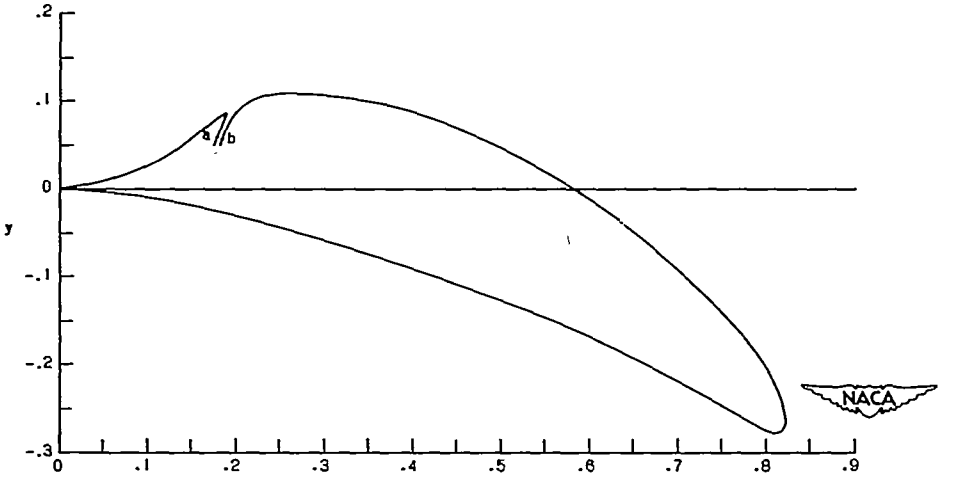

Figure 7. - First slotted blade with suction. Ratio of mass flows, m, -0.01; cascade spacing, d, 1.0488; upstream of cascade: magnitude of dimensionless velocity, q_1, 0.68215; angle of velocity, α_1, 135°; downstream of cascade: magnitude of dimensionless velocity, q_2, 0.42930; angle of velocity, α_2, 180°.

OTT2

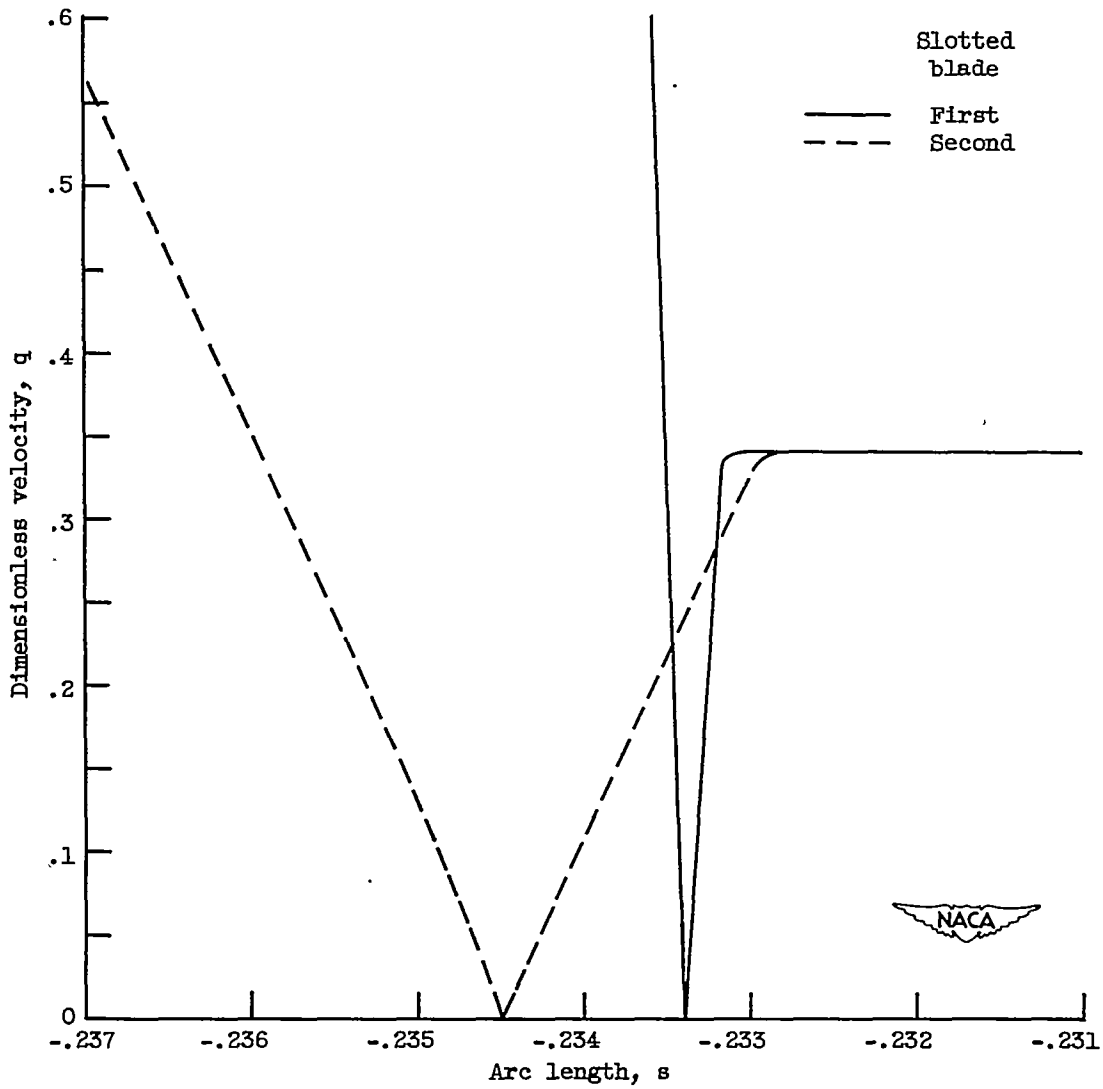

Figure 8. - Comparison of velocity distributions for first and second slotted blades in neighborhood of s_u.

2116

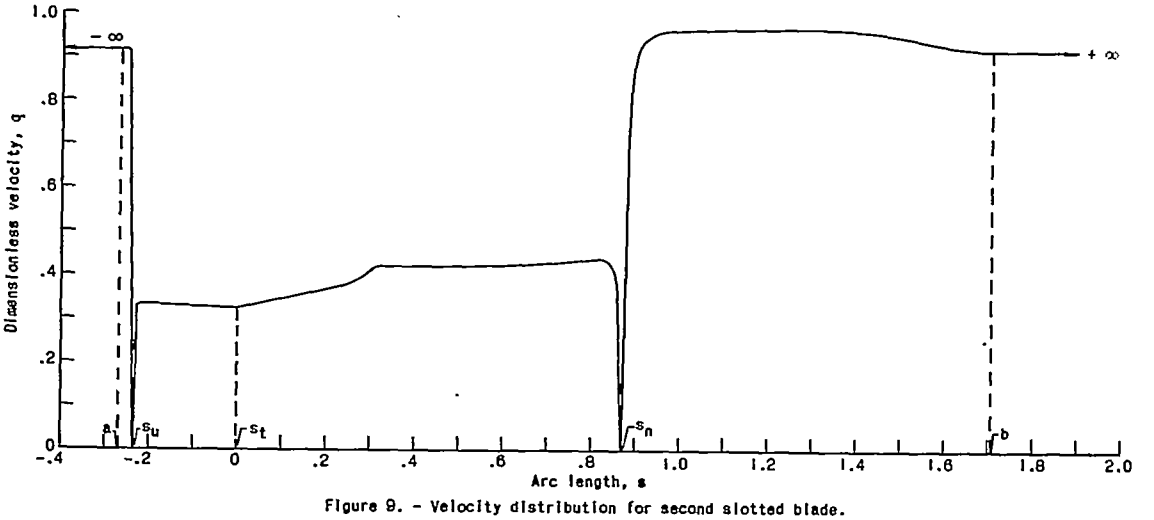

Figure 9. - Velocity distribution for second slotted blade.

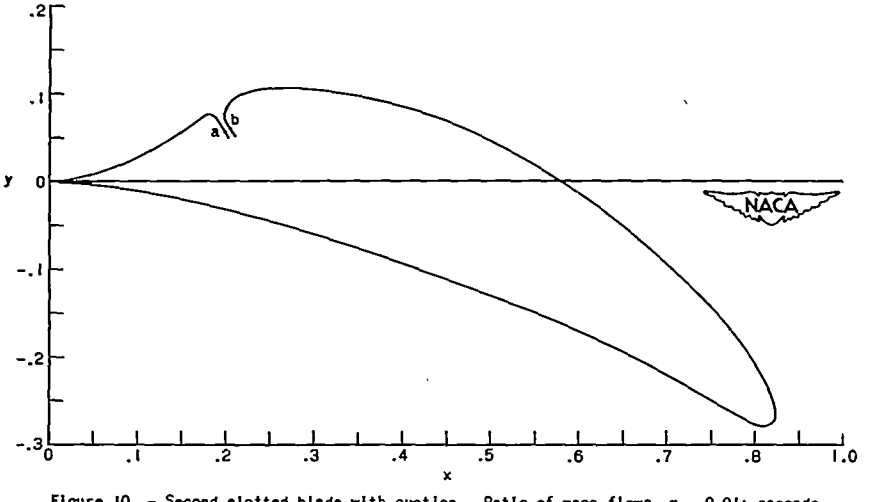

Figure 10. - Second slotted blade with suction. Ratio of mass flows, m, -0.01; cascade spacing, d, 1.0488; upstream of cascade: magnitude of dimensionless velocity, q_1, 0.68215; angle of velocity, α_1, 135°; downstream of cascade: magnitude of dimensionless velocity, q_2, 0.42930; angle of velocity, α_2, 180°.